Ultrasonic Transit-time Discharge Determination in Rectangular Open Channel

H. Hu[1], Z. Cheng[2], P. Gruber[3], Z. Wang[4*]

[1]National Institute of Metrology, Beijing, China
[2]Beijing Hydrology General Station, Beijing, China
[3]pgconsult, Switzerland
[4]China Institute of Water Resources and Hydropower Research, Beijing, China
[4]E-mail: bimonbird@163.com*

Abstract

Ultrasonic Transit-time method is a good choice to measure the open channel discharge. To investigate its performance in the rectangular open channels, a 26m long, 2m wide, 1.2m deep open channel facility was built with an over-fall head tank providing a very stable flowrate of 1.5m^3/s in maximum and 39 typical cases were tested. The tested results verified that ultrasonic transit-time method can be well used to measure the discharge in rectangular open channels. However, due to unavoidably disturbing the flow patterns and introducing some errors, thus the transducers should be made as small as possible to improve the measuring accuracy. In addition, more paths should be used to produce smaller errors. And at least two paths are suggested to be mounted in the range of h_i/H>0.7 to better reflect the influence of the free surface. Comparing sub-discharges in all zones, it can be found that substantial differences between mean-section method and Giordano Law exist below the lowest path. Larger K_b, for example 0.9, makes mean section method produce closer measurements to Giordano Law.

Key words: open channel, discharge determination, ultrasonic transit-time method, transducers' arrangement

1 Introduction

Discharge is a most important hydraulic parameter for open channels. Lots of different devices, including rated sections, ramp flumes, Parshall flumes, cutthroat flumes, weirs, are used to determine the flow discharges in open channels. Especially in the recent years, electromagnetic and ultrasonic Doppler flowmeters (Lynnworth and Liu, 2006), which are based on direct velocity measurements, have been rapidly developed and successfully applied in the open-channel's flow measurements. However, the discharge measuring accuracies are still not good enough. Heiner et al. (2011) evaluated the accuracies of multiple flow meters which were installed in various open channels, and the results showed two-thirds of the instruments exceeded the allowed errors with the maximum values being up to 40%. As high as 71% of the devices were unacceptable by visual inspection alone, and the reasons are mainly the improper site conditions couldn't fully meet the strict requirements. Therefore, in order to improve the accuracy of flowrate measurements in open channels, newly developed ultrasonic transit-time flowmeters maybe a very good alternative, due to their good stability and applicability (Hu et al. 2015).

As is well known, when travelling in the flow, the ultrasonic wave will take some time. And it will take some more time when travelling in the upstream direction than in the downstream direction due to the flow velocity. Based on this time difference, the flow velocity can easily be determined. Then, according to the velocities at different path heights, the flow rate can be obtained through numerical integration. This is the basic procedure of discharge determination with velocity measurements using ultrasonic transit-time method. Clearly, the discharge measuring accuracy is influenced by many factors, and the transducers' influence is one of them. In the actual fact, lots of works have been done in the discharge determination in pipes. Lüscher et al. (2007) analyzed the performance of ultrasonic transit-time method in pipes, and concluded that a higher number of acoustic paths could decrease the integration error, however they couldn't reduce the influence of the swirl or rotation. Hu et al. (2015) analyzed the influence of the swirl or transverse velocity to the line velocity measurements in a theoretical aspect and presented a mechanism analysis and estimation tool based on CFD. In addition, Zhang et al. (2011), Gruber et al. (2012), Hu et al. (2013), Zheng et al. (2014) examined the protrusion effects of transducers in the discharge determination in pipe flows. These researches also promoted the relative researches in open channels. Abgottspon et al. (2016) and ISO6416 (2005) presented a cross-path arrangement for transducers to counteract the influences of the transverse velocities. Cheng (2018) preliminarily analyzed the influences of the installing way of transducers. However, the quantitative assessment for transducers' influence on discharge determination is not fully conducted, and the influence mechanism is not comprehended yet. In addition, improvements of transducer arrangements, both economically and effectively, can also be promoted.

The integration method is another factor which can influence the discharge measurement largely. For pressure flows, the IEC 60041 standard (1991) proposed Gauss-Jacobi methods which was appropriate for circular pipes and the Gauss-Legendre method which was appropriate for rectangular conduits. These two methods are both built on the assumption that the path velocities are uniformly distributed, which in reality can't always be achieved. Thereafter, Tresch et al. (2008) improved the weights evaluation. Besides, velocity distributions were also integrated in the weight correction and optimal weighted integrations were proposed, with OWICS for circular section and OWIRS for rectangular section (Tresch et al., 2006; Lüscher et al., 2008). Staubli et al. (2008) used CFD results to improve the acoustic discharge measuring algorithm and made it suitable to the complex flow patterns. These researches also facilitate the study in open channel flows. ISO6416 (2005) provided a piecewise linear model to calculate the discharge coarsely, in which both the bottom velocity and the surface velocity were the keys. In order to more precisely illustrate the velocity distribution in open channels, Giordano (1995) proposed a combined form of power law and exponential law. Yang et al. (2004) examined the dip phenomenon in smooth uniform open channel and concluded that the location of the maximum velocity in a vertical profile in open channels is only dependent on the dip-correction factor α. Abgottspon et al. (2016) tried to incorporate the Giordano velocity profile to evaluate both key velocities. Han et al. (2018) proposed a calibration coefficient to minimize the systematic errors in discharge determination. However, systematic analysis on how to select integration method is still not available.

In this paper, the design and construction of a testing system is presented which allows to study the velocity determination and the improvement of the precision of ultrasonic transit-time flowmeters used for rectangular open channel measurements. Based on it, groups of experiments are conducted and analyzed. Especially both the transducers' influences and how to improve the arrangements are discussed. In addition, the integration methods are also studied, with the velocity distribution taken into consideration.

2 Principle of discharge determination

2.1 Line velocity measurement

An ultrasonic pulse travels in a downstream direction faster than a similar pulse travels upstream. The speed of a pulse travelling diagonally across the flow in a downstream direction will be increased by the velocity component of the water. Conversely, the speed of a pulse moving in the opposite direction will be decreased. If two transducers in pairs are mounted at the same elevation but on different sides and locations of the channel, as in Fig.1, the line velocity can be determined using the difference in the transit time in the two directions as Eq.1.

$$v_A = \frac{L}{2\cos\phi}\left(\frac{1}{t_2} - \frac{1}{t_1}\right) \tag{1}$$

in which, v_A is the line velocity; L is the path length (distance between transducer A and transducer B); ϕ is the angle between the path and direction of flow; t_1 is the transit time from transducer A to B; t_2 is the transit time from transducer B to A.

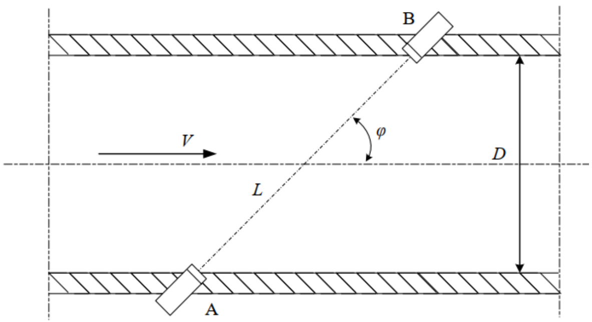

Fig.1 Schematic illustrating the line velocity determination

2.2 Discharge determination

Based on the line velocities at different elevations, the channel discharge can be determined with the help of an integration algorithm. Up till now, the integration algorithm mostly used in open channels is the mean-section method

(ISO6416, 2005). In this method, the whole cross section beneath the surface is divided into three types of sub-layers: top layer, middle layers and bottom layer, as in Fig.2.

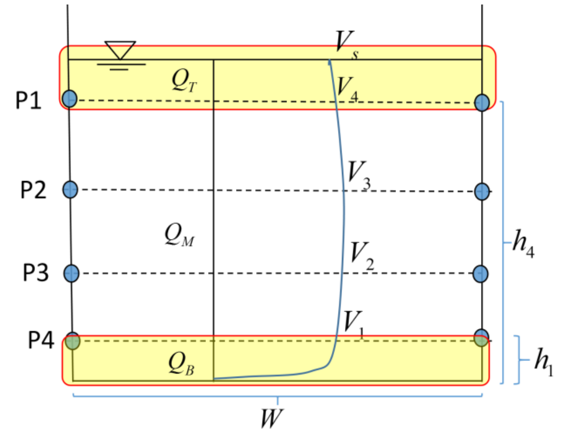

Fig.2 Mean-section method for rectangular channel

In the top layer, the mean velocity is calculated from a limited extrapolation of the line velocities of the top two paths. In the middle layers, the mean velocities are calculated from the two line velocities measured by the paths which bound the layer. In the bottom layer, the mean velocity is calculated according to the velocity measured by the lowest path and the near-bed velocity. The near-bed velocity is commonly determined empirically. Then the sub-discharges of each layer can be determined with the layer area evaluated as the mean values of the corresponding layer, as are shown in Eq.2~Eq5.

$$Q = \sum_{i=1}^{n+1} Q_i \tag{2}$$

For $i = n+1$

$$Q_{n+1} = 0.5\left(W_n + W_t\right)\left(h_t - h_n\right)\frac{v_n + K_t v_t}{1+K_t} \tag{3}$$

For $i = 2,3,\ldots,n$

$$Q_i = 0.25\left(W_{i-1} + W_i\right)\left(h_i - h_{i-1}\right)\left(v_{i-1} + v_i\right) \tag{4}$$

For $i = 1$

$$Q_1 = 0.25 h_1\left(W_1 + W_0\right)\left(v_1 + K_b v_1\right) \tag{5}$$

in which, Q is the total discharge; Q_i is the sub-discharge of i-th layer; W_i is the distance wall to wall of i-th path; W_0 is the width at channel bed; W_t is the width at flow surface; h_i is the height of i-th path from the channel bed; h_t is the height of the flow surface; v_i is the line velocity of i-th path; v_s is the line velocity at flow surface which can be obtained by extrapolation as Eq.6 and Eq.7; K_t is surface factor chosen commonly between 0~1, sometimes negative values are also allowed; K_b is bottom factor normally between 0.4 and 0.8; Subscript i=1,2,…n represents the order of path from bottom.

If $h - h_n < h_n - h_{n-1}$

$$v_s = v_n + \left(v_n - v_{n-1}\right)\times\frac{h_t - h_n}{h_n - h_{n-1}} \tag{6}$$

If $h_t - h_n \geq h_n - h_{n-1}$

$$v_s = v_n + \left(v_n - v_{n-1}\right) \tag{7}$$

If we know the velocity profile, the discharge can also be calculated by an analytical integration method. Giordano Law (Giordano, 1995) provides an analytical expression for the line velocity profile for open channels (see Eq.8). It can be determined only if the parameter a, b and c are all calibrated using the measured line velocities. Then combining with the width $W(z)$ at different elevation z, the total discharge Q can be got using Eq.9.

$$v(z) = a\cdot\left(\frac{z}{h_t}\right)^c \cdot e^{-b\cdot\frac{z}{h_t}} \tag{8}$$

$$Q = \int_{z=0}^{h} W(z) v(z)\,\mathrm{d}z \tag{9}$$

3 Testing system

3.1 General design

The testing system was built in Daxing Experimental Base of China Institute of Water Resources and Hydropower Research (IWHR). It consisted of a water tank, inflow pipes, a stilling pool, a rectangular flume, a tail gate and a tail water collecting device, as is shown in Fig.3. The water tank has a volume of 7.0m × 6.0m × 13.0m (length × width × height) and can provide a high water head and a large stable discharge for the tests. Inflow pipes, made up of two iron pipes of diameter 500mm, then supply the flow to the stilling pool. Both the master ultrasonic flow meters for pipes and flow adjusting valves are installed in the inflow pipes. The master ultrasonic flow meters were both pre-calibrated using weighing methods in the laboratory as is shown in Table 1. Indication errors were for both meters well below 0.5%, and the repeatability was better than 0.1%, which indicated that the precision and stability could both fulfill requirements. The stilling pool is 10.0m×4.8m (length×width), and was designed to dissipate energy and provide stable flow for the flume. The flume was designed with a size of 26.0m×2.0m (length×width), and its bottom was horizontal. The test sections were set 15m~20m downstream of the beginning of the flume. At the end of the flume, a tail gate was installed to adjust the water level in the flume. In addition, a drop of 0.4m was designed to avoid the tail water's back-propagation's influence.

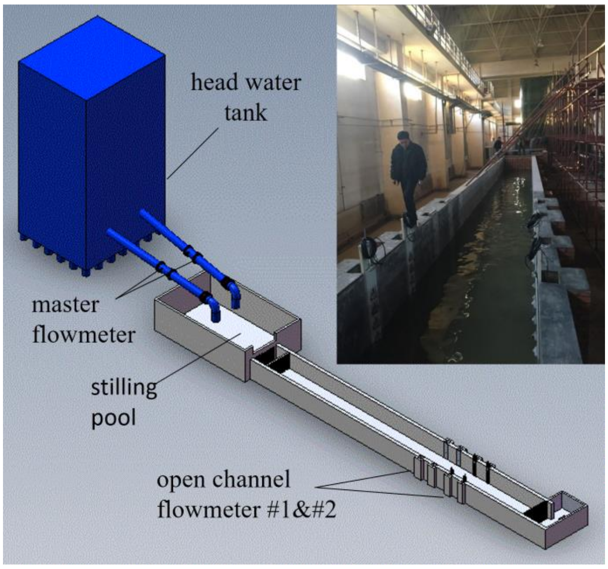

Fig.3 General design of the testing system

Table 1 Calibration of master flow meter

flow rate (m^3/h)	UF1(L) errors (%)	UF1(L) Repeatability (%)	UF2 (R) error (%)	UF2 (R) Repeatability (%)
1414	/	/	0.31	0.07
1060	-0.18	0.04	0.36	0.05
707	-0.09	0.08	0.38	0.07
353	-0.11	0.08	0.46	0.05
Average errors (%)	-0.13	/	0.38	/
Regulating factor	1.0013	/	0.9962	/

3.2 Ultrasonic flow meters in the open channel

In this testing system, two sets of ultrasonic transit-time flow meters were installed, and both were designed as crossed-path systems (see Fig.4). The upstream flow meter was labelled as No.1. Its mounting seats were made of aluminum, and were embedded in the pre-drilled troughs. Their outer surfaces were flush with the corresponding sidewalls, as is shown in Fig.5, to avoid disturbing flows. For flow meter No.1, at most eight pairs of transducers were planned to be installed in the seats, which is shown in Fig.5a. They are all small cylinders with diameters of 15mm. In addition, the path angles were designed as 60°. The downstream flow meter is labelled as No.2. Its mounting seats were installed similar to flow meter No.1. However, the transducers of flow meter No.2 are much bigger. They are semispherical with diameters of 30mm. Only 5 pairs were fixed in the mounting seats (see Fig.5b). Additionally the transducers can be placed in a protruded or recessed position as can be seen in Figure 5b.

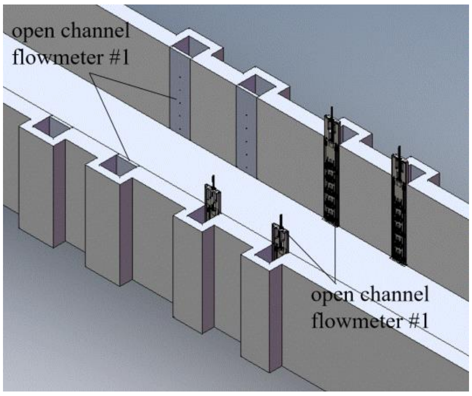

(a) Flowmeter position

Flowmeter #1 layer no	Flowmeter #1 path height	Flowmeter #2 layer no	Flowmeter #2 path height
P8	822	/	/
P7	722	/	/
P6	622	/	/
P5	522	P5	845
P4	422	P4	655
P3	322	P3	465
P2	222	P2	275
P1	122	P1	85

(b) path height (mm)

Fig. 4 Open channel flowmeters under test

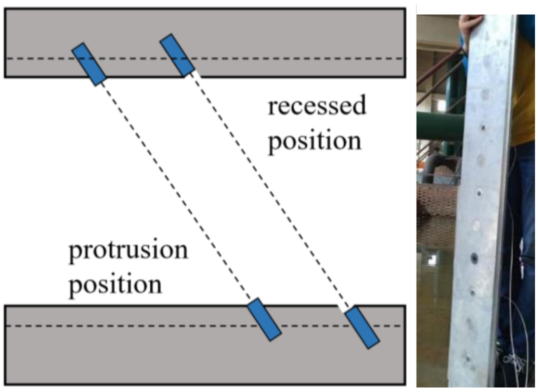

(a) Small transducer (No.1)

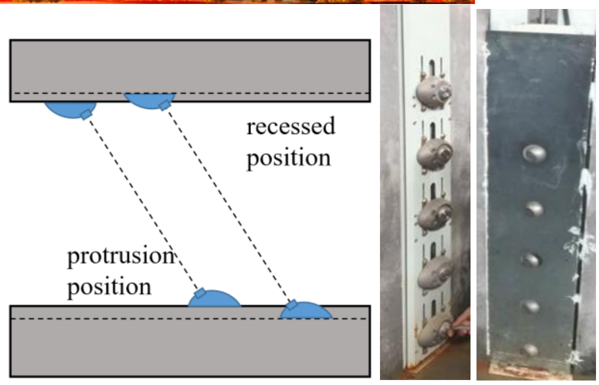

(b) large transducer (No.2)

Fig. 5 Transducer installation of tested flow meters

3.3 Parameter determination

The geometrical parameters, such as flume width W, transducer installing height h_i, acoustic path length L_i, and water level are all of great importance in the open channel discharge determination using ultrasonic flow meter. The water level was determined by an ultrasonic water level meter. The other parameters were all measured using a FARO arm and analyzed using POLYWORKS. In details, the side walls and the bottom are fitted by points measured using the FARO arm while the distance between the side walls is calculated by POLYWORKS. If the transducer positions are adjusted, the geometrical parameters will be refreshed.

(a) photo of geometric measurement

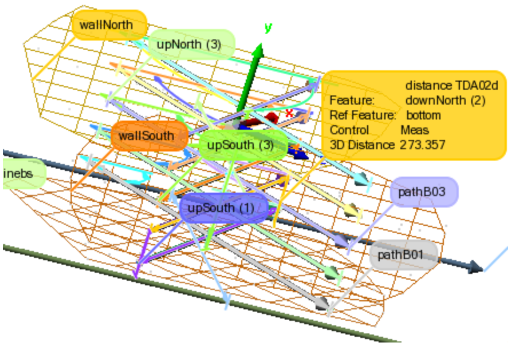

(b) geometric result showed in POLYWORKS

Fig. 6 Sketch of geometrical measurement

4 Results and discussions

4.1 Transducer shapes

Commonly transducers, accompanied with their protective coatings, are made like a semi-spherical shape. They are always set inside the channel and definitely occupy some space. In order to illustrate the influence of the transducers' occupation, 7 groups of tests were conducted. The discharges covered a range of 1300~3600m^3/h with the flow depths being 0.4m~1.0m. In these tests, both the two master flow meters were used to indicate the flows which passed through corresponding inflow pipes. The sums of their measurements reflected the total discharges Q in the flume, and are shown in Column 2 in Table 2. h_t represents the total flow depth.

In addition, both sets of open channel ultrasonic flow meters were used to indicate the discharges in the flume. For flow meter No.1, all the transducers were specially designed. In case 1 and case 2, the transducers were protruding into the flume, while in other cases, the transducers were retracted in the seats. The integration algorithm used in all cases was the mean-section method which is described in detail in ISO6416 (2005) and section 2.2 above. K_t was evaluated as 0.1 while K_b took the value of 0.4. The discharge readings Q_r are shown in column 4, and their corresponding measurement error ε, defined as in Eq.10, are shown in column 5. For flow meter No.2, the transducers were made like a semi-sphere, and occupied more space than those in flow meter No.1. The integration algorithm used is the same as that of flow meter No.1. The detailed results of flow meter No.2 are shown in column 7 and column 8.

$$\varepsilon = \frac{Q_r - Q}{Q} \times 100\% \qquad (10)$$

Q_r represents the discharge measurement of the tested flow meter.

Table 2 Tested cases and measurement errors of flow meter No.1 & No.2

Case No. (1)	Q (m^3/h) (2)	h_t (m) (3)	Flow meter No.1			Flow meter No.2		
			Q_r (m^3/h) (4)	ε (5)	Transducer states (6)	Q_r (m^3/h) (7)	ε (8)	Transducer states (9)
1	1385.9	1.046	1391.4	0.39%	retracted	1436.7	3.67%	protruded
2	1396.5	0.844	1400.7	0.30%	retracted	1445.4	3.50%	protruded
3	1412.5	0.846	1421.1	0.60%	protruded	1469.1	4.01%	protruded
4	1412.6	0.846	1420.8	0.58%	protruded	1468.2	3.93%	protruded
5	1416.2	0.683	1430.9	1.04%	protruded	1471.0	3.87%	protruded
6	1415.1	0.683	1428.7	0.96%	protruded	1470.9	3.94%	protruded
7	1366.8	0.520	1379.1	0.90%	protruded	1414.3	3.48%	protruded

Table 3 Tested cases and line velocities of each path

Case No.	Q (m^3/h)	ε_1	h_t (m)	v_1 (m/s)	v_2 (m/s)	v_3 (m/s)	v_4 (m/s)	v_5 (m/s)	v_6 (m/s)	v_7 (m/s)	v_8 (m/s)
8	1500.819	0.50%	0.851	0.233	0.238	0.245	0.247	0.251	0.257	0.257	0.257
9	2426.366	0.75%	0.930	0.337	0.345	0.356	0.362	0.368	0.379	0.381	0.389
10	2699.328	0.49%	0.897	0.391	0.400	0.412	0.417	0.426	0.438	0.441	0.451
11	3363.608	0.33%	0.949	0.454	0.465	0.479	0.487	0.498	0.514	0.521	0.537
12	3505.288	0.53%	0.930	0.487	0.500	0.513	0.520	0.530	0.545	0.553	0.568
13	1374.462	-0.35%	0.789	0.229	0.234	0.243	0.246	0.250	0.257	0.255	--
14	1381.112	-0.31%	0.653	0.280	0.286	0.296	0.303	0.310	0.319	--	--
15	2413.577	1.00%	0.568	0.567	0.585	0.606	0.618	0.624	--	--	--
16	1354.648	1.60%	0.416	0.366	0.377	0.391	0.394	--	--	--	--
17	1362.486	1.58%	0.501	0.449	0.463	0.475	--	--	--	--	--

Note: v_i represents the line velocity of i^{th} path from the bottom

According to Table 2, it can be concluded that the transducers' sizes play an important part in the discharge measurements. Clearly the bigger the transducers are protruding into the flume, the more their influences are. For flow meter No. 1, although the transducers are made very small, their influences are still apparent depending on their way of mounting. When the transducers are retracted in the seats, they only produce an average measurement error of 0.35%. However, when the transducers are protruding into the flume, the average measurement error increases more than double to 0.82%. If the transducer size is much larger, protruding into the flume produces much more measurement errors. For flow meter No.2, the transducers are much larger than those of flow meter No.1 with the diameter of 15mm, and produce as large measurement errors as 3.50~4.01%. In order to analyze the mechanism, a numerical simulation using Ansys Fluent is conducted and the result is shown as Fig.7. It can be seen that larger transducers will occupy more space, and will disturb the flows around the transducers more heavily. Clearly it will influence the time measurements and thus the discharge measurement. Besides, transducers can also cause the overestimation of the path length. In these physical model tests, a protrusion of 1mm can make an error of about 0.05% in path length. Thus to minimize the measurement errors of discharges, the transducers should be made small, and should be retracted in the mounting seats if possible. In addition, in order to give an accurate analysis as possible, flow meter No.1 was chosen to conduct further tests, and small transducers were retracted in the mounting seats.

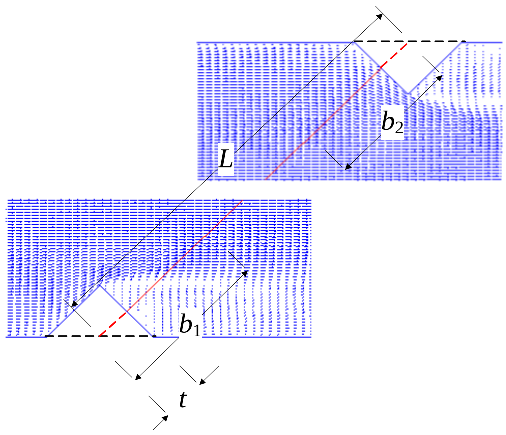

Fig.7 Transducers' protrusion disturbing the flow patterns

4.2 Path configurations

Theoretically, with more paths in use, the more accurate discharge measurements are obtained, if all paths are mounted properly. In this section, 10 typical cases were chosen to analyze the path configuration. The flow depths in cases 8 to 12 were large and so all 8 paths were in operation. And in cases 13 to 17, the flow depths were smaller and therefore less than 8 paths could be used. The line velocities of each path were measured and calculated based on cross-paths systems, and the detailed results are shown in Table 3. To plot the line velocities as a function of the path elevation in a dimensionless form results in Fig.8. V represents the average value of all the measured line velocities in the corresponding case.

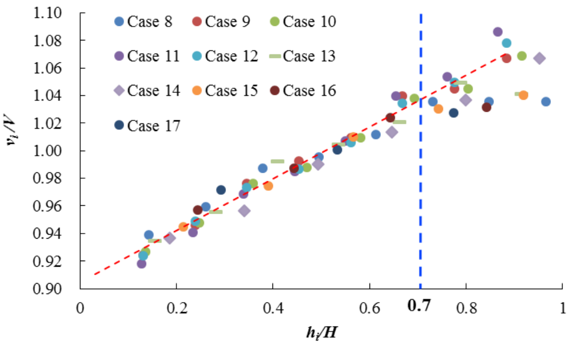

Fig.8 Line velocity upon mounting elevation in a dimensionless form

From Fig.8, it can be seen that when h_t/W_t<0.45 dimensionless velocity v_i/V increases with the dimensionless height h_i/h_t for all investigated cases. However, the rate of increase of v_i/V performs differently depending on h_i/h_t. When h_i/h_t is larger than 0.7, the rate of increase of v_i/V gets diffused with increasing h_i/h_t. The corresponding line velocities are generally smaller than the predicted values which would be obtained by extrapolation of the rate of increase of the line velocities of the underlying paths. Therefore if both top paths are lying in the range $h_i/h_t<0.7$, the surface velocity by extrapolation based on the top two paths may be too large, which would partly contributed to the positive error of discharge measurements. In case 16 and case 17, only one path is lying in the range of $h_i/h_t>0.7$, and the extrapolation of the surface velocity using the top two paths may also generate relatively larger prediction errors. Thus at least two paths should be mounted in the range $h_i/h_t>0.7$ to minimize the error produced by the surface velocity estimation. Through further analysis it is believed that the above phenomenon is caused by the influence of the free surface. Yang et al. (2004) proposed a method to determine the influence scope of the free surface using Eq.11

$$\frac{h_m}{h_t} = \frac{1}{1+\alpha} \tag{11}$$

in which, h_m is the distance of the maximum velocity point from the bed, and h_t-h_m is the influence depth of the free surface; α is the only parameter and can be estimated by Eq.12 in this paper.

$$\alpha = 1.3\exp\left(-\frac{W_t}{2h_t}\right) \tag{12}$$

Substituting hydraulic parameters of Case 8~17 can obtain that α is lying in the range of 0.117~0.453 and the corresponding h_m/h_t is within 0.688~0.895. In addition, the value of h_m/h_t decreases with the increasing flow depth when the channel wide is fixed. Clearly the minimum value of h_m/h_t of 0.688 (≈0.7) in these cases verifies that the influence scope of free surface is in the range of h/h_t>0.7 and only at least two paths mounted in the range $h_i/h_t>0.7$ can well reflect the free surface's influence. For paths which are lying in the range $h_i/h_t<0.7$ and are not close to the bottom, vi/V depends approximately linearly on h_i/h_t. And theoretically the line velocities at this range could be fully derived according to the line velocities obtained by neighboring paths. In another word, only limited paths need to be arranged in this range. By contrast, for the range where h_i/h_t approaches 0, vi/V is influenced not only by neighboring path velocities, but also by the boundary layer at the bottom. In order to estimate the velocity profile in this range, maybe more paths can be mounted or the integration algorithm can be improved. For the cases of $h_t/W_t \geqslant 0.45$, the critical value of 0.7 in this physical model tests might be improper and should be reevaluated. However, the division methods of the flow is still valid, as the flow mechanism keeps unchanged. If the method proposed by Yang et al. (2004) is used, α can be increased to the maximum of 1.3 and therefore the critical value can be decreased to the minimum of 0.435. However, the absolute value can be obtained only when h_t/W_t is determined.

In addition, transverse velocities were also unavoidably included in the path velocities due to diagonal planes, such as Case 8 with its transverse velocity distribution shown in Fig.9. In order to indicate the influence of the transverse velocity, Fig.10 is presented with v_y representing the transverse velocity and v_x representing the longitudinal velocity. Clearly the velocity along the path line should be measured as $v_x\cos\phi$ assuming v_y=0. However, the transverse velocity will exert an influence on the line velocity measurement. For the transducers of Group A, the measured line velocity will be added by $v_y\sin\phi$. When calculating longitudinal velocity v_A, the influence of transverse velocity will be divided by cosφ, which is shown as Eq.13. For the transducers of Group B, v_B can be obtained similarly as Eq.14.

$$v_A = \left(v_x \cos\phi + v_y \sin\phi\right)/\cos\phi \\ = v_x + v_y \tan\phi \qquad (13)$$

Clearly the flow velocities derived from the measured line velocities are not accurate enough, and unavoidably the influence of transverse velocity is included. However, if transducers of Group B are used as in Fig.10, the calculated longitudinal velocity v_B can be expressed as Eq.14. Combining Eq.13 and Eq.14 can derive Eq.15, and v_x can be obtained with influence of v_y being counteracted.

$$v_B = \left(v_x \cos\phi - v_y \sin\phi\right)/\cos\phi \\ = v_x - v_y \tan\phi \qquad (14)$$

$$v_x = \left(v_A + v_B\right)/2 \qquad (15)$$

In the actual fact, the transverse velocities are always large, especially the inflow conditions are not good enough. For Case 8, the largest transverse line velocity has a maximum value of 3.7% of the corresponding average line velocity in flow direction. Thus a crossed-path system is suggested if possible.

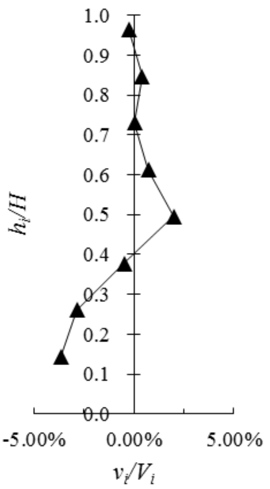

Fig.9 Transverse line velocities for case 8

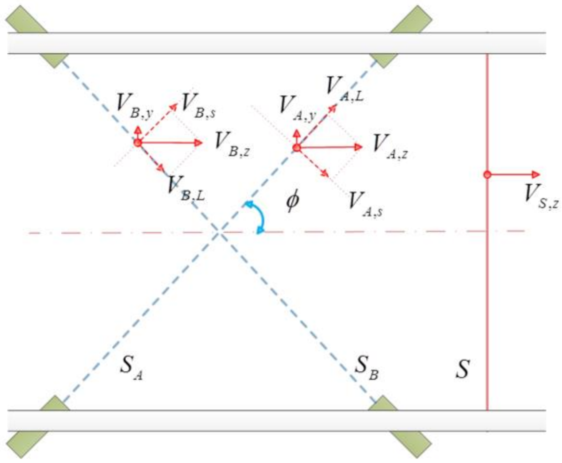

Fig.10 Sketch of influence of transverse flow

4.3 Integration method

The integration method decides how the line velocity distribution on the flow depth is approximated. This approximation will unavoidably lead to some measurement errors. In this section, another 22 groups of tests (39 groups in all) are presented using flow meter No.1 (small transducers), to make discharge measurements. Both the mean-section methods (MSM) and the Giordano law approximation method (GL) were applied to the raw data derived from the velocity measurements of the investigated flow meter as shown in Fig.10. In this figure, case 9 and case 15 are taken as examples for further analysis. The black and red solid polylines represent the line velocity profiles obtained by the mean-section method and parameter K_t was set to 0.1 while K_b to 0.4. The surface and bottom velocities were not obtained by measuring, but extrapolated using the neighbor line velocities. The blue and grey dashed curves represent approximated velocity profiles based on Giordano Law using the least square method. It can be seen clearly that in the intermediate layers, the velocity profiles obtained by the mean-section method and the Giordano Law approximation can fit well with each other. The main differences mainly occur in the top and the bottom layers. The approximations of the top layer are lying above the corresponding top paths while the bottom layer are lying below the corresponding lowest paths. Both integrated methods produce different velocity profiles in these two layers, thus producing different integration errors.

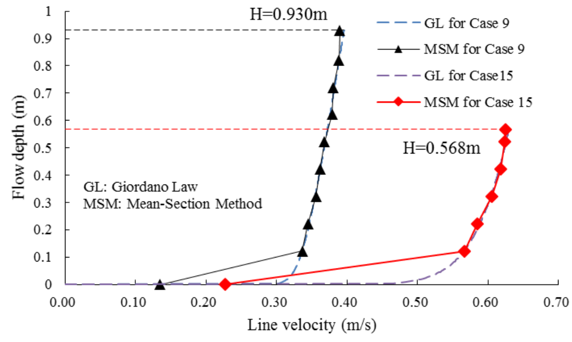

Fig.11 Mean-section method and Giordano Law to describe the line velocity profile for two typical cases (9,15)

Line-velocity profile characteristics vary depending on the elevations. Therefore when conducting an error analysis for the discharge evaluation, the total flow depth can be divided into three parts. The flow below the lowest path is named Part I. The flow above the top path is named Part III. Part II is lying between Part I and Part III. In order to make a comprehensive analysis, all the 39 cases are used.

For Part II, both the mean-section method and the Giordano Law method produce accurate sub-discharge determinations. However, as the integration methods are different, the sub-discharges calculated by these two methods are not exactly the same. In this section, the sub-discharges of Part II Q_{II} were calculated for all the 39 cases using both integration algorithms. The results, as shown in Fig.12, indicate that the sub-discharge differences Δ_{II} are very small, less than 0.1% of the total discharges in the corresponding cases. And more paths produce smaller sub-discharge differences Δ_{II} between two integration methods. The reason for the small errors in three-path cases might result from compensation effects of the approximation.

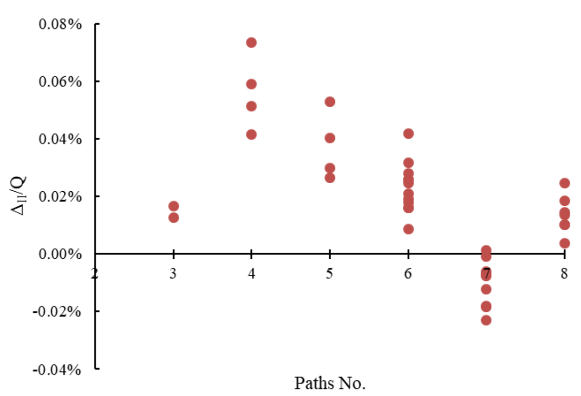

Fig.12 Sub-discharge differences of the mean-section method and the Giordano Law method for Part II

For Part I, the Giordano Law method can give well-defined sub-discharges while the mean-section method will provide a series of values for each case depending on the choice of K_b. Thus, the results of both methods might differ more. In this section, both methods are used. Especially for the mean-section method, K_b commonly takes values in the range of 0~1 according to the ANSI 6416 norm (ISO 6416 2005). Thus 9 values between 0.1 and 0.9 with an interval of 0.1 between them are chosen. The results are all shown in Fig.13, in which Δ_I represents the differences of the calculated results by both methods and Δ_I/Q indicates their relative measurement errors over corresponding total discharge. Clearly, the more paths are mounted, the smaller the differences of both algorithms are. And Δ_I/Q is strongly related with K_b. For the investigated cases, the differences between the two algorithms are getting smaller with the increasing K_b, with K_t evaluated as 0.1. When K_b takes an inappropriate value, such as 0.1, mean-section method and Giordano Law could generate differences larger than 10% of the corresponding total discharges. For the tested cases, values of K_b around 0.9 show relatively small differences between the mean-section method and Giordano Law in evaluating sub-discharges of Part I. In a word, the accuracy of Q_I's evaluation can greatly influence the determination of total discharges, thus K_b should be optimized when using the mean section method.

Fig.11 shows the line-velocities and the paths' elevations. Clearly the lowest path is still in the main flow region. And its line-velocity may not reflect the characteristics of line velocities in Part I. So choosing K_b was done by experience. Thus in order to evaluate K_b as well as the sub-discharge of Part I as well as possible, the lowest path position should be lowered and the line-velocities in the boundary at the bottom should be known. The lowering must however take into account that reflexion on the bottom might lower the reliability of determining the lowest path.

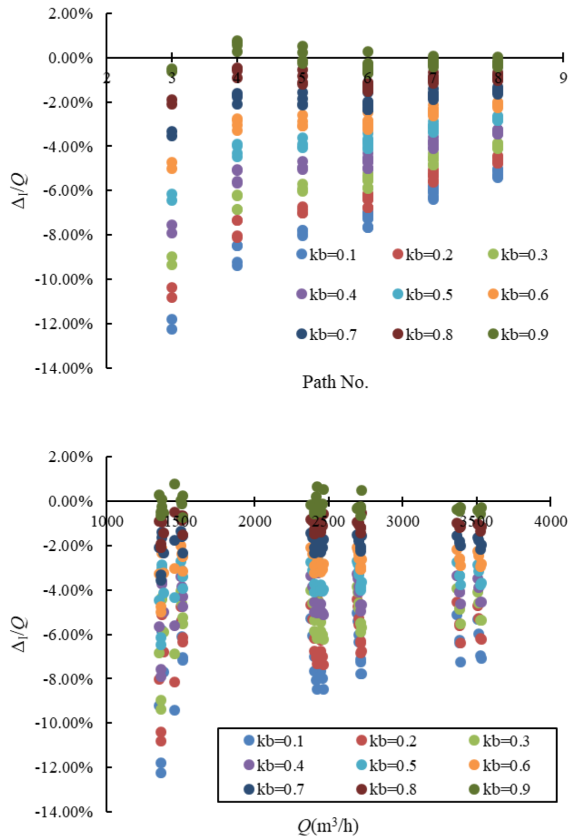

Fig.13 Sub-discharge differences of mean-section methods and Giordano Law for Part I

For Part III, the Giordano Law uses the line-velocity profiles above the top path according to the fitted curve by all installed paths, and the sub-discharges in Part III are also obtained by numerical integration of the analytical profile (equation 8). In contrast, the mean-section method uses surface velocity by linear extrapolation based on the top two paths. Therefore, the line-velocity profiles of the two integration methods are different, leading to different sub-discharges of Part III. Additionally, as the flow surface varies depending on the height difference H-h_t the choice of K_t is difficult and might be made dependent on H-h_t. In this measurement campaign, K_t is evaluated in the range of 0.1 to1.0, and all the 39 cases are used to further analysis. The results are shown in Fig.14, and Δ_{III} represent the sub-discharge differences of both methods for each case.

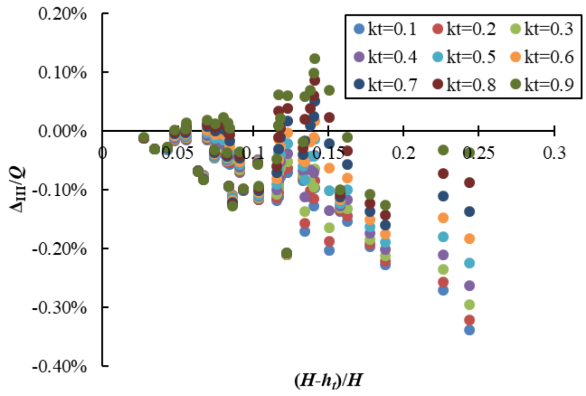

Fig.14 Sub-discharge differences of mean-section methods and Giordano Law for Part III

From Fig.14, it can be seen that if $(H$-$h_t)/H$ is small, the relative error Δ_{III}/Q was also small and the choice of K_t has little influence on Δ_{III}/Q (see $(H$-$h_t)/H<0.15$). That's because for these cases, the water level is close to the installation height of the top path: the top layer is always rather thin and the sub-discharge of Part III is only a small portion of the total flow. As $(H$-$h_t)/H$ gets larger, the top layer gets thicker, and the corresponding sub-discharge of Part III gets larger. Any small changes of K_t produce in these cases, relatively large errors Δ_{III}/Q. Taking the conclusions obtained by Fig.8 into considerations, one can conclude that in order to obtain relative accurate measurements of sub-discharge of Part III, enough paths should be arranged in the depth range $h_i/H>0.7$ and $(H$-$h_t)/H$ should be minimized if possible. Here too, the top path cannot be too close to the water level due to the ultrasonic reflexion on the water surface. If the water level is not constant during the operation of the channel, switch on and off strategies have to be implemented

Comparing Part I, Part II and Part III, it can be concluded that the sub-discharges differences in Part II are small between Giordano Law and mean section method. However, for Part III, the sub-discharges differences in Part III are a little larger. In comparison, the sub-discharges in Part I show substantial differences between two methods. Improper evaluation for K_b in mean section method can produce as large discharge differences as 12% from Giordano Law, especially in cases of small discharges. Thus, it was very important to properly determine K_b.

5 Conclusions

The Ultrasonic transit-time method is widely used for the discharge determination in open channels. In order to verify the performance of ultrasonic transit-time flow meters and to analyze their errors, a testing system was designed and 39 cases were tested. The main conclusions are as follows:

1) The Ultrasonic transit-time method can be used to determine the discharge in open channels.

2) The transducers of ultrasonic open channel flow meters always protrude into the channel and therefore disturb the local velocity field, which introduces some errors in the determination of the discharge. Thus the transducers should be made as small as possible, and be mounted into the corresponding side walls if possible. This effect is more dominant in smaller channels as the one used in this test study. Compensation methods are complicated and need detailed flow field measurements or simulation around the transducers.

3) More paths produce smaller errors if properly mounted. It is better to mount at least two paths in the range of $h_i/H>0.7$ in order to accurately extrapolate the line velocity profile at the surface, and the height difference H-h_t should not be too large.

4) Integration methods play an important part in the determination of the discharge in open channels. In this paper, the Giordano Law and mean-section methods (ISO6416) were used for further analysis. The results of the tests show that the sub-discharges between the top path and the lowest path are largely identical but with minor differences between two methods. The sub-discharges differences above the top path can be narrowed if the distance between surface and top path height is reduced. However, the Giordano Law and mean-section methods show substantial differences in the determination of sub-discharges below the lowest path. Especially the sub-discharge determination by the mean-section method varies greatly with K_b. Commonly large K_b, for example 0.9, could produce small difference from the Giordano Law.

Acknowledgments

This paper is currently supported by The National Key R&D Program of China “Research and application of national quality infrastructure” (project/subject SN. 2017YFF0206303) and National Natural Science Foundation of China (51909278) .

Reference

[1] Abgottspon A, Staubli T, Gloor N. (2016). Open channel discharge measurement using the acoustic transit time method – a case study. IGHEM.

[2] Cheng X. (2018). Influence of transducer protrusion on the accuracy of flow measurement in open channels by ultrasonic transit-time method. Tsinghua University, Beijing China. (in Chinese)

[3] Giordano P. (1995). Il Calcoco della portata nei canali a pelo libero a partire da misure di velocita media trasversale. ENEL, Italy.

[4] Gruber P, Wermelinger F, Deschwanden F. (2012). Influence of protrusion effect on the accuracy of the acoustic discharge measurement. IGHEM.

[5] Han J, Shao J, Fu W, et al. (2018). Study of ultrasonic flowmeter method for open channel flow calculation. South-to-North Water Transfers and Water Science & Technology, 16(2): 196-201. (in Chinese)

[6] Heiner B, Barfuss S L, Johnson M C. (2011). Conditional Assessment of Flow Measurement Accuracy. Journal of Irrigation & Drainage Engineering, 137(6):367-374.

[7] Hu H, Zhang L, Meng T, etc. (2015). Mechanism analysis and estimation tool of flow error due to disturbed flow filed for multipath ultrasonic flowmeter. ISFFM, Arlington, U.S.

[8] Hu Y, Zhang T, Zheng D, et al. (2013). Estimation on influence of probe protrusion length of ultrasonic flowmeteron measurement. Journal of Tianjin University (Science and Technology), 46(9): 776-783. (in Chinese)

[9] IEC 60041. (1991). International Code for the Field Acceptance Test to determine the hydraulic performance of hydraulic turbines, storage, pumps and pump turbines.

[10] ISO 6416. (2005). Hydrometry– Measurement of discharge by the ultrasonic (acoustic) method. BS EN

[11] Lüscher B, Staubli T, Tresch T, et al. (2007). Accuracy analysis of the acoustic discharge measurement using analytical, spatial velocity profile. Hydro: 373-379

[12] Lüscher B, Staubli T, Tresch T, et al. (2008). Optimizing the acoustic discharge measurement for rectangular conduits. IGHEM.

[13] Staubli T, Luescher B, Gruber P, et al. (2008). Optimization of acoustic discharge

measurement using CFD. International Journal on Hydropower & Dams, 15(2): 109-112.

[14] Tresch T, Gruber P, Staubli T. (2006). Comparison of integration methods for multipath acoustic discharge measurements. IGHEM.

[15] Tresch T, Luescher B, Staubli T. (2008). Presentation of optimized integration methods and weighting corrections for the acoustic discharge measurement. IGHEM.

[16] Lynnworth L，Liu Y，Ultrasonic flowmeters: Half-century progress report, 1955–2005. (2006). Ultrasonics, 44: 1371-1378.

[17] Voser A, Staubli T. (1996). CFD calculations of the protrusion effect and impact on the acoustic discharge measurement accuracy. IGHEM.

[18] Yang S, Tan S, Lim S. (2004). Velocity distribution and dip-phenomenon in smooth uniform open channel flows. Journal of Hydraulic Engineering, 130(12): 1179-1186.

[19] Zhang P, Zheng D, Xu T, et al. (2011). Study on the influence of ultrasonic probes on flow field and measurement performance of ultrasonic flowmeter. Journal of Experiments in Fluid Mechanics, 25(3): 60-65. (in Chinese)

[20] Zheng D, Zhao D, Zhang P. (2014). Study on mechanism of flow disturbance caused by acoustic transducers in flow measurement. Journal of Mechanical Engineering, 50(4): 18-24. (in Chinese)